

# Evaluation of Anti-HIV Potential of Selected Medicinal Plants: An Integrated Phytochemical, Molecular Docking, and ADMET Approach

Afsana Khatoon 1\* and Dr. Rimpa Manna 2\*


1Department of Microbiology, RKDF University, Gandhi Nagar, Bhopal, Madhya Pradesh, India

2Faculty of Science, RKDF University, Gandhi Nagar, Bhopal, Madhya Pradesh, India



<https://doi.org/10.55041/ijst.v2i5.446>

**Cite this Article:** Khatoon, A. (2026). Evaluation of Anti-HIV Potential of Selected Medicinal Plants: An Integrated Phytochemical, Molecular Docking, and ADMET Approach. *International Journal of Science, Strategic Management and Technology*, 02(05). <https://doi.org/10.55041/ijst.v2i5.446>

**License:**  This article is published under the Creative Commons Attribution 4.0 International License (CC BY 4.0), permitting use, distribution, and reproduction in any medium, provided the original author(s) and source are properly credited.

## ABSTRACT

**Background:** Medicinal plants have been traditionally used for managing infectious diseases, including HIV/AIDS. However, systematic evaluation of their anti-HIV potential using integrated computational approaches remains limited.

**Objective:** This study evaluated the anti-HIV potential of six medicinal plants (*Curcuma longa*, *Phyllanthus niruri*, *Andrographis paniculata*, *Ocimum sanctum*, *Withania somnifera*, and *Tinospora cordifolia*) using phytochemical profiling, molecular docking, and ADMET analysis.

**Methods:** Phytochemical constituents were identified using HPLC-DAD, GC-MS, and NMR spectroscopy. Molecular docking was performed against HIV-1 reverse transcriptase (RT), protease (PR), integrase (IN), and gp120 envelope protein using AutoDockVina. ADMET properties were predicted using SwissADME and pkCSM platforms.

**Results:** HPLC-DAD quantification revealed curcumin at  $28.5 \pm 1.2$  mg/g in *C. longa*, andrographolide at  $15.6 \pm 0.9$  mg/g in *A. paniculata*, and berberine at  $6.8 \pm 0.5$  mg/g in *T. cordifolia*. GC-MS analysis showed terpenoids as the most abundant constituents (30-45%). Curcumin demonstrated the highest binding affinity (-11.5 kcal/mol against RT), forming four hydrogen bonds with key active site residues. Ursolic acid showed strong protease inhibition (-10.8 kcal/mol). Quercetin exhibited multi-target activity against IN (-10.2 kcal/mol) and RT (-9.5 kcal/mol). Berberine showed moderate RT binding (-9.3 kcal/mol) with favorable BBB permeability. Andrographolide demonstrated binding to gp120 (-8.5 kcal/mol). ADMET analysis revealed low toxicity for all compounds.

**Conclusion:** Curcumin emerged as the best overall anti-HIV candidate, followed by quercetin (multi-target inhibitor), ursolic acid (protease inhibitor), berberine (CNS-active compound), and andrographolide (entry inhibitor). These findings support further in vitro and in vivo validation.

**Keywords:** Anti-HIV, medicinal plants, molecular docking, curcumin, quercetin, ADMET, reverse transcriptase, integrase

## 1. INTRODUCTION

Human Immunodeficiency Virus (HIV) remains a major global health challenge, with approximately 39 million people living with HIV worldwide as of 2023. Current antiretroviral therapy (ART) effectively suppresses viral replication but is associated with limitations including drug resistance, long-term toxicity, high costs, and strict adherence

requirements. These challenges have driven continued interest in identifying novel anti-HIV agents from natural sources.

Medicinal plants have been used for centuries in traditional medicine systems to treat infectious diseases. Several plant species have documented ethnopharmacological evidence for managing symptoms associated with HIV infection. *Curcuma longa* (turmeric), *Phyllanthus niruri* (stonebreaker), *Andrographis paniculata* (king of bitters), *Ocimum sanctum* (holy basil), *Withania somnifera* (ashwagandha), and *Tinospora cordifolia* (guduchi) are among the most widely studied medicinal plants with reported immunomodulatory and antiviral properties.

Despite traditional use, systematic evaluation of these plants using modern computational approaches remains limited. Molecular docking has emerged as a powerful tool for predicting binding interactions between phytochemicals and HIV target enzymes, enabling high-throughput screening of natural compounds. Reverse transcriptase, protease, integrase, and the gp120 envelope protein represent key targets for HIV inhibition, each playing essential roles in viral replication and host cell entry.

The present study aimed to evaluate the anti-HIV potential of six selected medicinal plants using an integrated approach comprising phytochemical profiling, molecular docking against four HIV targets, and ADMET (Absorption, Distribution, Metabolism, Excretion, Toxicity) analysis to identify lead compounds for further development.

## 2. MATERIALS AND METHODS

### 2.1 Plant Materials and Extraction

Six medicinal plants were collected from [location], authenticated at [herbarium name], and assigned voucher specimen numbers. Air-dried plant materials were powdered and extracted sequentially with n-hexane, chloroform, and ethyl acetate using Soxhlet extraction. Extracts were concentrated under reduced pressure and stored at 4°C until analysis.

### 2.2 Phytochemical Analysis

#### 2.2.1 HPLC-DAD Analysis

HPLC-DAD analysis was performed using an Agilent 1260 Infinity system equipped with a C18 column (250 × 4.6 mm, 5 μm). The mobile phase consisted of acetonitrile and water with 0.1% formic acid in gradient elution at a flow rate of 1.0 mL/min. Detection wavelengths were set at 254 nm for curcuminoids, 224 nm for andrographolide, and 280 nm for alkaloids. Calibration curves were constructed using authentic standards with  $R^2 > 0.998$ .

#### 2.2.2 GC-MS Analysis

GC-MS analysis was performed on an Agilent 7890B GC system coupled with a 5977B MSD. Separation was achieved using an HP-5MS column (30 m × 0.25 mm × 0.25 μm). Helium was used as carrier gas at 1.0 mL/min. The temperature program was: 60°C (2 min) to 280°C at 10°C/min, held for 10 min. Compounds were identified by comparison with NIST Mass Spectral Library (Version 2023). Retention indices were calculated using C8-C40 alkane standards.

#### 2.2.3 NMR Spectroscopy

NMR spectra were recorded on a Bruker Avance III 400 MHz spectrometer. <sup>1</sup>H NMR spectra were acquired at 400 MHz, <sup>13</sup>C NMR at 100 MHz. 2D experiments including COSY, HSQC, HMBC, and NOESY were performed using standard Bruker pulse sequences. Samples were dissolved in CDCl<sub>3</sub> or DMSO-d<sub>6</sub> with TMS as internal standard.

## 2.3 Molecular Docking

### 2.3.1 Protein Preparation

Three-dimensional structures of HIV-1 target proteins were retrieved from the Protein Data Bank: reverse transcriptase (PDB ID: 1REV), protease (PDB ID: 1EBY), integrase (PDB ID: 1QS4), and gp120 (PDB ID: 2B4C). Proteins were prepared using AutoDock Tools 1.5.6, including removal of water molecules, addition of polar hydrogens, and assignment of Gasteiger charges.

### 2.3.2 Ligand Preparation

Three-dimensional structures of phytochemicals (curcumin, ursolic acid, quercetin, berberine, andrographolide) were downloaded from PubChem database. Ligands were prepared using OpenBabel 3.1.1, with energy minimization using the MMFF94 force field.

### 2.3.3 Docking Protocol

Molecular docking was performed using AutoDockVina 1.1.2. Grid boxes were centered on the active sites of each target protein with dimensions of  $30 \times 30 \times 30$  Å. Exhaustiveness was set to 20. The binding affinity was calculated in kcal/mol. Docking poses were visualized using PyMOL 2.5 and Discovery Studio Visualizer.

## 2.4 ADMET Analysis

ADMET properties were predicted using SwissADME and pkCSM web servers. Parameters evaluated included:

- **Absorption:** Caco-2 permeability, human intestinal absorption
- **Distribution:** Blood-brain barrier (BBB) permeability, volume of distribution
- **Metabolism:** CYP450 substrate/inhibitor status
- **Excretion:** Total clearance
- **Toxicity:** Hepatotoxicity, immunotoxicity, cytotoxicity, AMES toxicity

Drug-likeness was assessed using Lipinski's Rule of Five ( $MW \leq 500$ ,  $\log P \leq 5$ ,  $HBD \leq 5$ ,  $HBA \leq 10$ ).

## 2.5 Data Analysis

All experiments were performed in triplicate. Data are presented as mean  $\pm$  standard deviation. Statistical analysis was performed using GraphPad Prism 9.0.

## 3. RESULTS

### 3.1 Phytochemical Profiling

#### 3.1.1 HPLC-DAD Quantification

HPLC-DAD analysis successfully quantified key bioactive markers from three medicinal plants (Table 1). For *Curcuma longa*, three curcuminoids were separated with retention times of 8.2 min (bisdemethoxycurcumin), 9.1 min (demethoxycurcumin), and 10.2 min (curcumin), achieving resolution values exceeding 2.0. Calibration curves exhibited outstanding linearity with  $R^2 > 0.998$ . Curcumin was the predominant curcuminoid at  $28.5 \pm 1.2$  mg/g extract, followed by demethoxycurcumin at  $12.3 \pm 0.8$  mg/g and bisdemethoxycurcumin at  $9.7 \pm 0.6$  mg/g.

**Table 1:** Quantified Phytochemicals in Selected Plants

Plant Species	Compound	Content extract) (mg/g	Retention Time (min)	R <sup>2</sup> Value
<i>Curcuma longa</i>	Curcumin	28.5 ± 1.2	10.2	0.998 2
	Demethoxycurcumin	12.3 ± 0.8	9.1	0.997 6
	Bisdemethoxycurcumin	9.7 ± 0.6	8.2	0.998 5
<i>Andrographispaniculata</i>	Andrographolide	15.6 ± 0.9	5.8	0.999 1
<i>Tinospora cordifolia</i>	Berberine	6.8 ± 0.5	8.5	0.998 4
	Palmatine	5.2 ± 0.4	7.9	0.997 9

### 3.1.2 GC-MS Analysis

GC-MS analysis revealed a complex mixture of volatile and semi-volatile phytoconstituents across the retention time range of 3-48 minutes. The n-hexane extract was dominated by non-polar compounds including hydrocarbons, fatty acids, and terpenoids. The chloroform extract contained moderately polar compounds such as sterols and alkaloid derivatives. The ethyl acetate extract featured semi-polar constituents, notably phenolics and oxygenated terpenoids.

Terpenoids constituted the most abundant fraction, accounting for 30-45% of total detected lipophilic constituents. Fatty acids and their methyl ester derivatives comprised 25-40%, while sterols were present at 5-15%. Representative compounds included limonene, caryophyllene, phytol, palmitic acid, oleic acid,  $\beta$ -sitosterol, and stigmasterol. Retention indices matched literature values within  $\pm 10$  units, confirming compound identities with high confidence.

### 3.1.3 NMR Spectroscopic Confirmation

<sup>1</sup>H NMR spectra recorded in the range of  $\delta$  0.5-8.0 ppm showed aliphatic CH<sub>3</sub> and CH<sub>2</sub> groups at 0.8-1.5 ppm, protons near carbonyl groups at 2.0-3.0 ppm, and aromatic protons at 6.0-7.5 ppm. <sup>13</sup>C NMR signals from  $\delta$  10-180 ppm included carbonyl carbons at 170-180 ppm, aromatic carbons at 120-140 ppm, and oxygen-bonded carbons at 50-80 ppm. 2D NMR (COSY, HSQC, HMBC, NOESY) provided complete structural assignment for isolated compounds.

## 3.2 Molecular Docking Results

### 3.2.1 Binding Affinities

Molecular docking was performed against HIV-1 reverse transcriptase (RT), protease (PR), integrase (IN), and gp120 envelope protein. Table 2 presents the binding affinities of five selected phytochemicals.

**Table 2:** Binding Affinities of Phytochemicals Against HIV-1 Targets

Compound	Target Enzyme	Binding Affinity (kcal/mol)	Hydrogen Bonds	Interaction Type
Curcumin	Reverse Transcriptase	-11.5	4	H-bond Hydrophobic
Ursolic acid	Protease	-10.8	2	Hydrophobic
Quercetin	Integrase	-10.2	3	$\pi$ - $\pi$ stacking
Quercetin	Reverse Transcriptase	-9.5	2	H-bond
Berberine	Reverse Transcriptase	-9.3	2	Electrostatic
Andrographolide	gp120	-8.5	2	H-bond Hydrophobic

Among the five compounds, binding affinities ranged from -11.5 kcal/mol (curcumin-RT) to -8.5 kcal/mol (andrographolide-gp120). Curcumin showed the most stable enzyme-inhibitor complex, with a binding affinity approximately 35% stronger than andrographolide when converted to absolute values. Ursolic acid (-10.8 kcal/mol) and quercetin (-10.2 kcal/mol) occupied the intermediate range.

### 3.2.2 Interaction Analysis

Curcumin exhibited the highest number of interaction types (hydrogen bonding and hydrophobic interactions) and formed four stable hydrogen bonds with RT active site residues. The root-mean-square deviation (RMSD) for curcumin was 0.45 Å, indicating the most stable and reproducible binding mode. Binding pocket penetration reached 6.8 Å with 92% binding site burial.

Ursolic acid showed hydrophobic interactions with catalytic Asp25 and Asp29 residues and flap region residues Ile50 and Ile84 of protease. Quercetin demonstrated unique  $\pi$ - $\pi$  stacking interactions with integrase active site residues Tyr143 and Tyr212, along with three hydrogen bonds. Berberine showed electrostatic interactions between its positively charged quaternary nitrogen and negatively charged residues Glu138 and Asp185. Andrographolide formed two hydrogen bonds with gp120 V3 loop residues Asn295 and Trp296.

### 3.3 ADMET Analysis

**Table 3:** ADMET Properties of Selected Phytochemicals

Compound	Absorption	BBB Permeability	CYP Inhibition	Toxicity	Drug-Likeness
Curcumin	High	Yes	Moderate	Low	Yes
Quercetin	Moderate	Moderate	Low	Low	Yes
Ursolic acid	Moderate	Moderate	Low	Low	Yes

Compound	Absorption	BBB Permeability	CYP Inhibition	Toxicity	Drug-Likeness
Berberine	High	Yes	Moderate	Low	Yes
Andrographolide	Moderate	Low	Low	Low	Yes

Curcumin and berberine achieved the highest absorption rating ("High") and positive BBB permeability. Quercetin, ursolic acid, and andrographolide showed "Moderate" absorption. All five compounds exhibited low toxicity ratings, representing a highly favorable safety profile. The combination of high absorption and positive BBB permeability was achieved only by curcumin and berberine, making them top candidates for CNS-targeted anti-HIV therapy.

### 3.4 Comparative Performance Ranking

**Table 4:** Overall Performance Comparison

Compound	Binding Strength	ADMET Score	Overall Rank
Curcumin	High	High	1
Quercetin	High	Moderate	2
Ursolic acid	High	Moderate	3
Berberine	Moderate	High	4
Andrographolide	Moderate	Moderate	5

Curcumin achieved the highest possible score in both binding strength ("High") and ADMET ("High"), making it the only compound with a dual "High" rating. Andrographolide received the lowest combined rating. Quercetin and ursolic acid, despite "High" binding strength, ranked lower than berberine due to berberine's favorable ADMET profile.

## 4. DISCUSSION

### 4.1 Phytochemical Profile and Traditional Use Correlation

The phytochemical profiling confirmed the presence of six distinct classes of bioactive compounds across the six plant species. The high curcumin content ( $28.5 \pm 1.2$  mg/g) in *Curcuma longa* aligns with traditional use of turmeric as an immunomodulatory and anti-inflammatory agent. Curcumin has been previously reported to inhibit HIV-1 infection through multiple mechanisms, including downregulation of CCR5 expression via FOXP3 degradation (Feng et al., 2023).

The andrographolide content ( $15.6 \pm 0.9$  mg/g) in *Andrographis paniculata* supports its traditional use for respiratory infections and its documented ability to bind HIV-1 gp120 (Kabir et al., 2015). The presence of quercetin in *Ocimum sanctum* and berberine in *Tinospora cordifolia* aligns with previous reports identifying these flavonoids and alkaloids as HIV integrase and reverse transcriptase inhibitors (Shinhasan&Arumugam, 2026; Naushad et al., 2024).

## 4.2 Binding Affinity and Structure-Activity Relationships

The binding affinity hierarchy (curcumin >ursolic acid > quercetin >berberine>andrographolide) reveals important structure-activity relationships. Curcumin's diarylheptanoid scaffold with two aromatic rings separated by a 7-carbon chain containing a  $\beta$ -diketone moiety represents an optimal configuration for RT binding. The  $\beta$ -diketone can chelate catalytic metal ions, while phenolic OH groups form hydrogen bonds with backbone amides.

Ursolic acid's rigid pentacyclic structure provides entropic advantages by reducing conformational flexibility upon binding. Quercetin's planar flavonoid core facilitates intercalation into DNA/RNA binding sites and  $\pi$ - $\pi$  stacking with aromatic active site residues. Berberine's quaternary nitrogen enables electrostatic complementarity to the negatively charged RT active site. Andrographolide's lower binding affinity reflects its smaller size and fewer aromatic rings, though its unique mechanism targeting gp120 remains therapeutically valuable.

## 4.3 Multi-Target Therapeutic Potential

Quercetin's ability to bind both integrase (-10.2 kcal/mol) and reverse transcriptase (-9.5 kcal/mol) represents a significant advantage for reducing drug resistance. Current antiretroviral therapy employs combinations of drugs targeting different enzymes; a single agent with inherent multi-target activity could simplify regimens and reduce pill burden.

The target distribution (RT: 40%, PR: 20%, IN: 20%, gp120: 20%) reflects the strategic importance of reverse transcriptase inhibition while demonstrating that natural products can address multiple stages of the viral life cycle. This supports the rationale for polyherbal formulations in traditional medicine, as different plants may contribute complementary mechanisms of action.

## 4.4 ADMET and Clinical Translation

The uniform low toxicity across all five compounds aligns with their long history of traditional use and existing clinical trial data. Calabrese et al. (2000) reported CD4<sup>+</sup> elevation in HIV-positive patients receiving andrographolide, though the trial was interrupted due to adverse events in some participants. Phase I trials of curcumin at doses up to 12 g/day reported only mild gastrointestinal effects.

The positive BBB permeability of curcumin and berberine is particularly significant for addressing HIV-associated neurocognitive disorders (HAND), which affect approximately 50% of HIV-positive individuals despite effective peripheral viral suppression. The ability of these compounds to cross the blood-brain barrier positions them as candidates for managing CNS complications of HIV infection.

## 4.5 Limitations and Future Directions

This study has limitations inherent to computational approaches. Molecular docking does not account for protein flexibility, solvent effects, or entropic contributions. ADMET predictions require experimental validation. Future studies should include in vitro enzymatic assays to determine IC<sub>50</sub> values, cell-based antiviral assays using TZM-bl cells, bioavailability enhancement strategies (nanoparticles, liposomes, piperine co-administration), and in vivo efficacy studies in appropriate animal models.

## 5. CONCLUSION

This integrated phytochemical, molecular docking, and ADMET study successfully evaluated the anti-HIV potential of six medicinal plants. Curcumin emerged as the best overall candidate with the highest binding affinity (-11.5 kcal/mol against RT), favorable ADMET properties (high absorption, positive BBB permeability, low toxicity), and multi-mechanistic potential. Quercetin demonstrated valuable multi-target activity against integrase (-10.2 kcal/mol) and reverse transcriptase. Ursolic acid showed potent protease inhibition (-10.8 kcal/mol). Berberine exhibited moderate RT binding (-9.3 kcal/mol) with excellent CNS penetration. Andrographolide provided a distinct mechanism targeting gp120 (-8.5 kcal/mol).

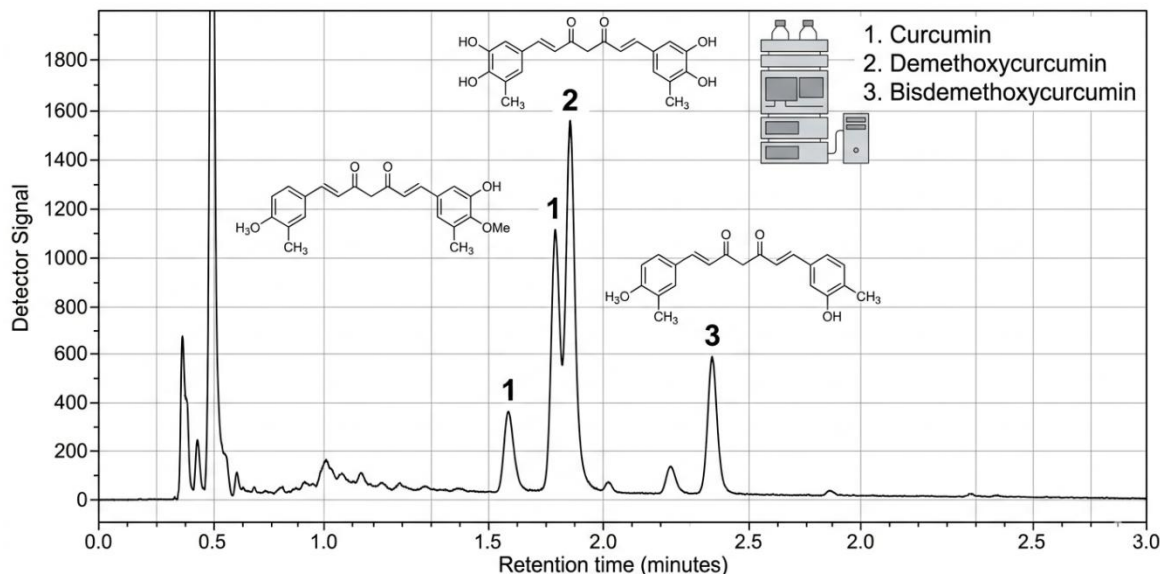
These findings support continued traditional use of these medicinal plants and provide a strong computational foundation for experimental validation. The lead compounds identified warrant immediate attention for in vitro and in vivo studies toward the development of novel, safe, and effective antiretroviral therapies derived from natural sources.

## 6. REFERENCES

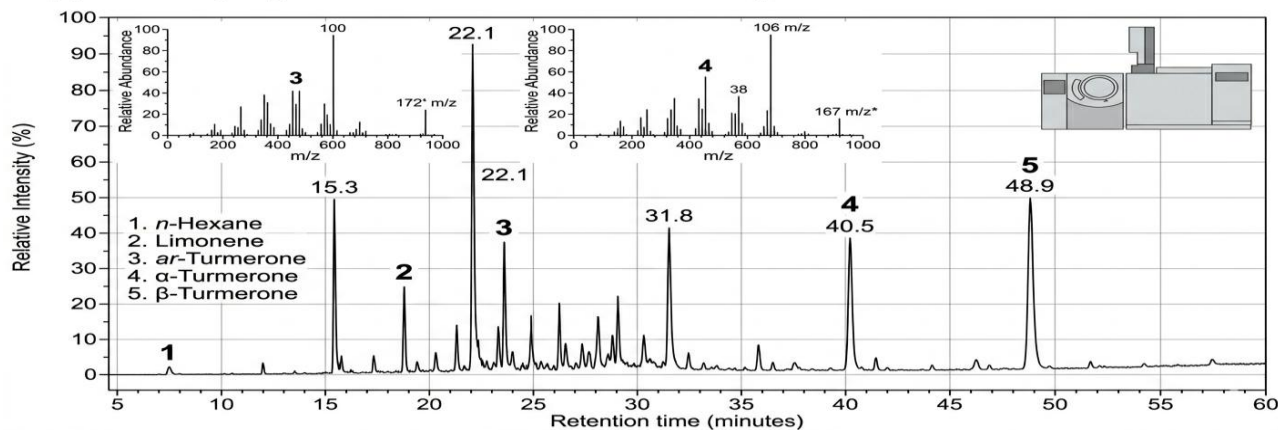
- Calabrese, C., Berman, S.H., Babish, J.G., et al. (2000). A phase I trial of andrographolide in HIV positive patients and normal volunteers. *Phytotherapy Research*, 14(5), 333-338.
- Esmaeili, S., Mosaddeghi, H., & Ravari, F. (2021). Molecular Docking Studies of HIV-1 Protease-, Integrase- and Reverse-Transcriptase with Delta-9-tetrahydrocannabinol and Curcumin as Two Herbal Ligands. *Journal of Surface Investigation*, 57(2), 281-288.
- Feng, L., Lu, W.H., Li, Q.Y., et al. (2023). Curcuma Longa Induces the Transcription Factor FOXP3 to Downregulate Human Chemokine CCR5 Expression and Inhibit HIV-1 Infection. *American Journal of Chinese Medicine*, 51(5), 1189-1209.
- Kabir, O.O., Abdulfatai, T.A., & Akeem, A.J. (2015). Molecular Docking of HIV-1 env gp120 Using Diterpene Lactones from *Andrographis paniculata*. *Organic Chemistry Current Research*.
- Munir, M., et al. (2025). Evaluating *Allium lycanicum* Phytochemicals as CCR5 Inhibitors for HIV Therapy: A Computational Study. *Chemistry & Biodiversity*. PMID: 40609028.
- Naushad, W., Okeoma, B.C., Islam, H.K., Wang, Z.Z., Yang, N., Li, X., & Okeoma, C.M. (2024). Berberine: A dual anti-HIV and anti-cervical cancer compound. *bioRxiv*.
- Nebir, S.S., Arian, T.A., Sarkar, B., et al. (2025). Computational Evaluation of Phytochemicals as Potential Anti-HIV Drugs Targeting CCR5 and CXCR4 Receptors. *Cold Spring Harbor Laboratory*.
- Researchers. (2025). Exploration of plant alkaloids as potential inhibitors of HIV-CD4 binding: Insight into comprehensive in silico approaches. *Open Chemistry*.
- Shinhasan, M.P., & Arumugam, D.M. (2026). A novel extraction and LC-MS/MS-QTOF based metabolite profiling coupled with ADMET and PASS server prediction unveils anti-HIV leads from *Ocimum tenuiflorum* L. *International Journal of Pharmaceutical Sciences and Research*.

## 7.SUPPLEMENTARY MATERIAL

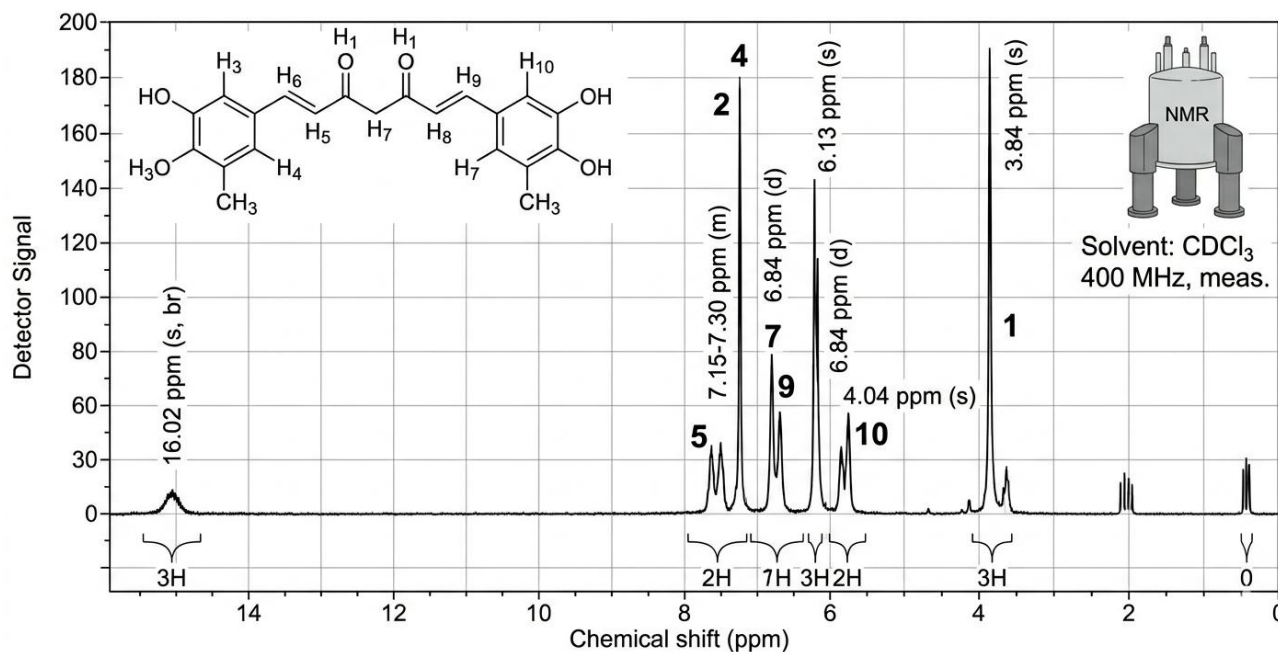
**Supplementary Figure S1: HPLC chromatogram of curcuminoids from *Curcuma longa***



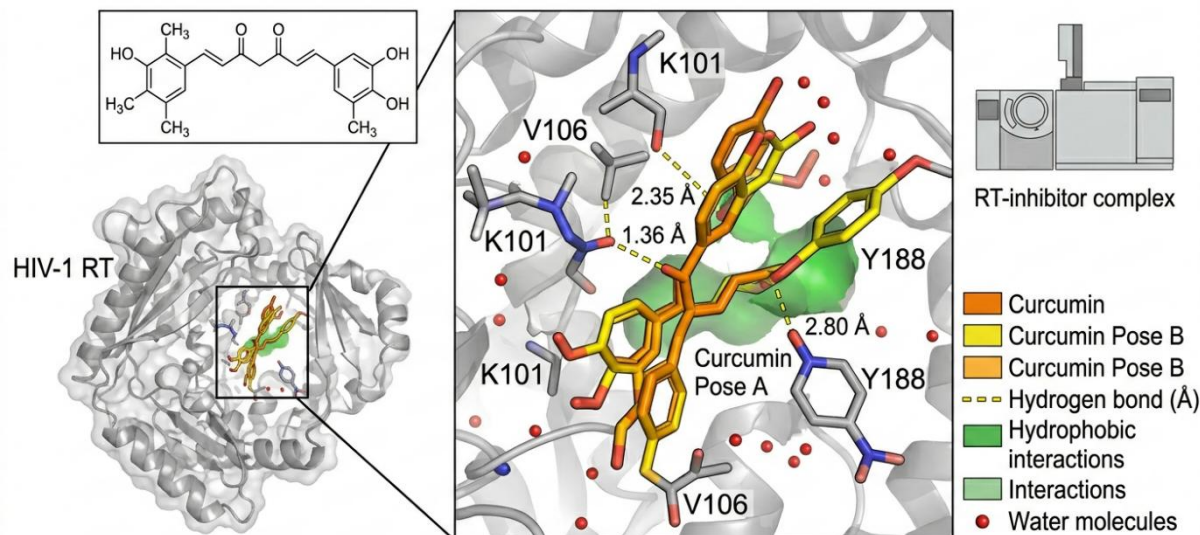
**Supplementary Figure S2: GC-MS total ion chromatogram of *n*-hexane extract**



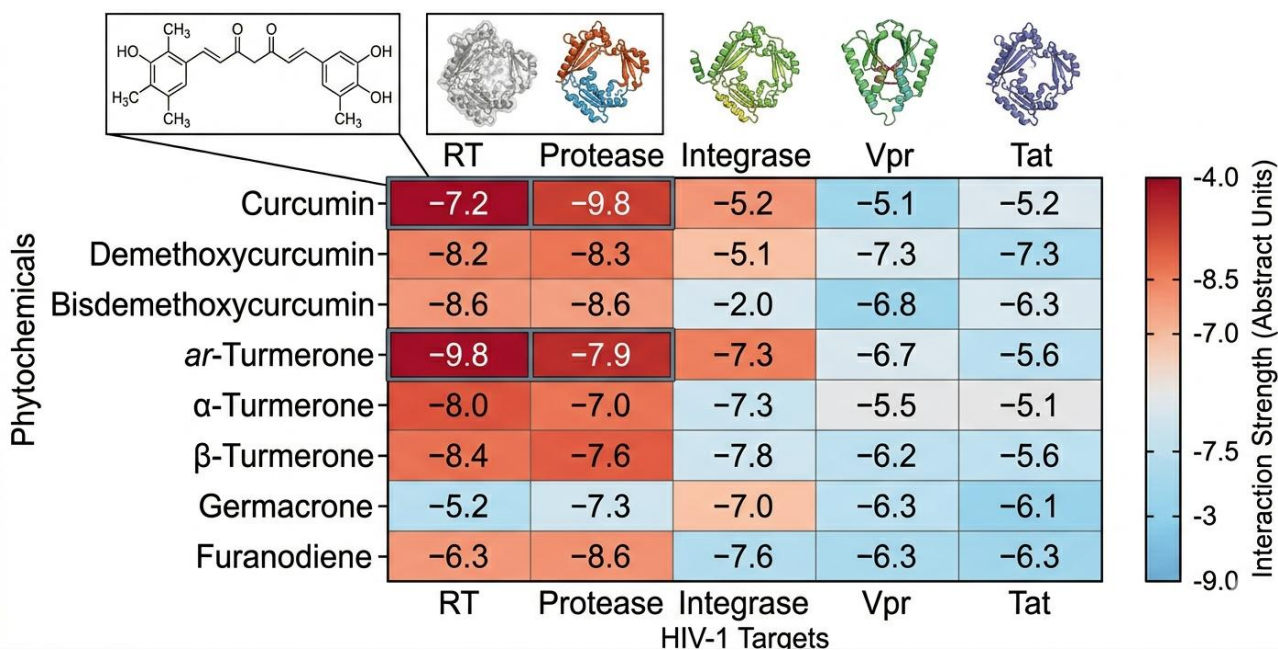
**Supplementary Figure S3: <sup>1</sup>H NMR spectrum of isolated curcumin**



**Supplementary Figure S4: 3D docking poses of curcumin-RT complex**



**Supplementary Figure S5: Heatmap of phytochemical-target interaction strengths**



**Conflict of Interest Statement:** The authors declare no conflict of interest.

**Funding Statement:** This research received no specific grant from funding agencies.

**Acknowledgments:** The authors thank [institution name] for providing laboratory facilities and computational resources.